

Characteristics of Gas Flow within a Micro Diffuser/Nozzle Pump *

LI Xiu-Han(李修函)¹, YU Xiao-Mei(于晓梅)^{1**}, ZHANG Da-Cheng(张大成)¹, CUI Hai-Hang(崔海航)²,
LI Ting(李婷), WANG Ying(王颖)¹, WANG Yang-Yuan(王阳元)¹

¹Institute of Microelectronics, Peking University, Beijing 100871

²Institute of Mechanics, Chinese Academy of Sciences, Beijing 100080

(Received 18 January 2006)

The gas flow characteristics for various shapes of micro diffuser/nozzles have been experimentally investigated. The micro diffuser/nozzles with the lengths of $70\text{ }\mu\text{m}$, $90\text{ }\mu\text{m}$, $125\text{ }\mu\text{m}$ and the taper angles of 7° , 10° , 14° are designed and fabricated based on silicon micromachining technology for optimizing and comparing. The flat-wall diffuser/nozzle is $40\text{ }\mu\text{m}\times 5\text{ }\mu\text{m}$ in depth and width. An experimental setup is designed to measure the gas flow rates under controlled temperature and pressure condition. Optimized values for the taper angle and the length of the diffuser/nozzle are experimentally obtained.

PACS: 47.60.+i, 47.17.+e, 47.45.-n

Micro diffuser/nozzle pumps utilize different pressure drop characteristics of flow through a diffuser and a nozzle to direct the flow in one preferential direction, and hence cause a net pumping direction. Major advantages of micro diffuser/nozzles are that the risk of wear and fatigue in passive check valves is eliminated and that the danger of valve clogging is reduced.^[1] Many extensive studies have been conducted on the diffuser/nozzle problems experimentally, analytically and numerically.^[2-4] For example, low Reynolds effects have been studied by Manton^[5] in their diffuser/nozzle pumps for a steady incompressible flow. Caen^[6] studied compressible flow in a diffuser/nozzle pump, but without considering rarefaction effects. Dorrepaal^[7] presented an analytical solution for incompressible flows in diffuser/nozzles with slip at wall, while this slip was not due to rarefaction effects. Recently Aubert^[8] analysed the unsteady gaseous slip flows in diffuser/nozzles numerically. Although the geometry of the diffuser/nozzle is very simple, some parts of the physical laws governing the fluid flow in micro diffuser/nozzle remain unknown. The flow mechanism is very complex, and the diffuser/nozzle design is still mainly based on experimental results.

The diffuser/nozzles have been tested to work for several pumps with different sizes and pump modes.^[9-11] As vacuum suction mode can effectively decrease the formation of air bubbles and overcome the interface tension between liquid and solid wall in the micro-fluidic systems,^[12] gas pumping is a good way for liquid filling in microchip. In such micro diffuser/nozzle pumps, the Knudsen numbers are generally located in the slip flow and transitional-flow regimes.^[13] Therefore, the gas flow performance of the micro diffuser/nozzle was studied both experimentally and theoretically.

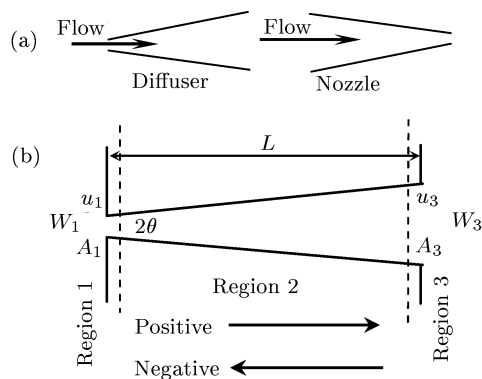


Fig. 1. Definitions of the diffuser and the nozzle.

A diffuser is a conduit with an expanding cross-sectional area in the flow direction intended to reduce velocity in order to recover the pressure head of the flow. A nozzle is a conduit with decreasing cross sectional area in the flow direction (Fig. 1(a)). The pressure drops across the diffuser/nozzle can be divided into three parts, as illustrated in Fig. 1(b), namely the pressure drop at the entrance (region 1), the pressure drop within the diffuser/nozzle (region 2), and the expansion loss of the pressure drop at the exit of the diffuser/nozzle (region 3).^[14] In Fig. 1(b), L and 2θ are the length and the taper angle of the diffuser/nozzle, while u_n , A_n , and W_n denote the velocity, the cross section area and the width of the different regions. Based on our previous experimental results, the Reynolds number Re and Mach number Ma of the fluid, which determine the flowage, were calculated to be nearly 60 and 0.1, respectively. Hence the fluid flow in the experiment belongs to laminar current and the Bernoulli equation could be used.

The total pressure drop, which is the sum of the

* Supported by the National Natural Science Foundation of China under Grant No 90207013, and the National High Technology Research and Development Programme of China under Grant No 2002AA404420.

** To whom correspondence should be addressed. Email: yuxm@ime.pku.edu.cn

©2006 Chinese Physical Society and IOP Publishing Ltd

pressure drops across the different regions, in the positive diffuser direction ΔP_{diff} and the negative nozzle direction ΔP_{nozzle} can be written as

$$\Delta P_{\text{diff}} = \Delta P_{d1} + \Delta P_{d2} + \Delta P_{d3}, \quad (1)$$

$$\Delta P_{\text{nozzle}} = \Delta P_{n1} + \Delta P_{n2} + \Delta P_{n3}, \quad (2)$$

where subscripts 1, 2, and 3 denotes regions 1, 2 and 3; and subscripts d and n denote diffuser and nozzle. The pressure drop ΔP at a given position is usually expressed by

$$\Delta P = \frac{1}{2} K \rho \bar{u}^{-2}, \quad (3)$$

where K is the pressure loss coefficient at corresponding regions, ρ is the fluid density, and \bar{u} is the upstream mean velocity at this position. According to the fluidic continuity equation, in the diffuser direction, $\bar{u}_1 \approx \bar{u}_2$, $\bar{u}_3 \approx \frac{A_1}{A_3} \bar{u}_1$, while in the nozzle direction, $\bar{u}_2 \approx \bar{u}_3 = \frac{A_1}{A_3} \bar{u}_1$. Using Eq. (3), Eqs. (1) and (2) can be rewritten as

$$\Delta P_{\text{diff}} = \left[K_{d1} + K_{d2} + K_{d3} \left(\frac{A_1}{A_3} \right)^2 \right] \frac{1}{2} \rho \bar{u}_1^2, \quad (4)$$

$$\Delta P_{\text{nozzle}} = \left[K_{n1} + (K_{n2} + K_{n3}) \left(\frac{A_1}{A_3} \right)^2 \right] \frac{1}{2} \rho \bar{u}_1^2. \quad (5)$$

Then the flow efficiency ratio η of a diffuser/nozzle can be expressed as^[15]

$$\eta = \frac{\xi_{\text{nozzle}}}{\xi_{\text{diff}}} = \frac{K_{n1} + (K_{n2} + K_{n3}) (A_1/A_3)^2}{K_{d1} + K_{d2} + K_{d3} (A_1/A_3)^2}, \quad (6)$$

where ξ_{nozzle} and ξ_{diff} are the total pressure loss coefficient for the nozzle and diffuser direction respectively. A_1 and A_3 are the cross sections at the entrance and exit of the diffuser/nozzle according to Fig. 1. The flow efficiency ratio η for a diffuser/nozzle has to be greater than one in a diffuser/nozzle pump. This means that the pressure loss for a given flow in the diffuser direction is lower than that in the nozzle direction if $\eta > 1$, while $\eta < 1$ will lead to pumping direction in the nozzle direction.

Figure 2 gives the working principle of a micro diffuser/nozzle pump. In the supply mode (Fig. 2(a)), as the volume of the pump chamber increases, more fluid enters the pump chamber from the element on the left, which acts as a diffuser, than that on the right, which acts as a nozzle. On the other hand, in the pumping mode (Fig. 2(b)) more fluid goes out of the element on the right which now acts as a diffuser, while the element on the left act as a nozzle. One cycle consists of a supply mode (a) and a pump mode (b). During one actuation period T , the net flow is formed from the left side to the right side. The average volume output

flow rate (Q) of the pump can be expressed as^[13]

$$Q = \frac{2\Delta V_m}{T} \frac{\sqrt{\eta} - 1}{\sqrt{\eta} + 1}. \quad (7)$$

where ΔV_m is the volume variation of the pump chamber. It can be seen from Eq. (7) that the pump performance depends strongly on the η value of a diffuser/nozzle. If $\eta > 1$, then $Q > 0$, and the fluid will enter the pump cavity from the port A and pump out from the port B, hence the net flow is formed from port A to port B.

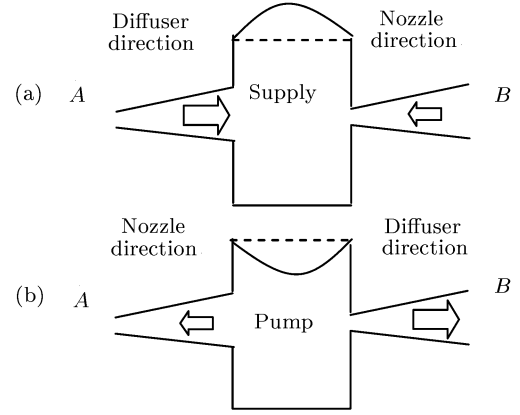


Fig. 2. Operations of diffuser/nozzle pump in one cycle: (a) supply mode, (b) pump mode.

In order to characterize the micro diffuser/nozzle, we have employed designs on two factors, namely the length and the angle of the diffuser/nozzle (see Fig. 1), and each factor has three levels. Table 1 gives the design parameters of the diffuser/nozzles and calculated value of η . The diffuser/nozzles are with rectangular (flat-walled) cross-section, sharp-edged entrances. The width and the depth of the narrow entrances for all diffuser/nozzles are designed to be $5 \mu\text{m} \times 40 \mu\text{m}$, and the calculated area ratios A_1/A_3 are listed in Table 1. The information available to calculate η is based on the theoretical results that are given by Olsson *et al.*^[16] In the diffuser direction, $K_{d1} = 0.5$, $K_{d2} = 0.05$, and $K_{d3} = 1$ for exits are regardless of the shape of the exit region. In the nozzle direction, $K_{n1} = 1.0$, $K_{n2} = 0.01$, $K_{n3} = 0.5$.

The diffuser/nozzles and the pumps were fabricated with a simple micromachining processes using two-steps of deep etching techniques. The first etching step formed the pump chambers with KOH anisotropic etch. The second etching was performed under a deep reactive ion etching (DRIE) system, which formed the diffuser/nozzles with the depth of $40 \mu\text{m}$. The silicon wafers were anodic bonded to a glass wafer that has inlet/outlet holes opened. Figure 3 shows an optical image of a finished micro diffuser/nozzle pump and an SEM photo of the diffuser/nozzle.

Table 1. Geometric configuration of the test diffuser/nozzles according to Fig. 1.

Diffuser/ nozzle	Throat width W_1 (μm)	Diffuser/ nozzle length L (μm)	Taper angle θ	η	Deepness (μm)	Shape of cross section	A_1/A_3
Group 1	5	70	14°	1.70	40	Rectangle	0.23
		90		1.75			0.18
		125		1.77			0.14
Group 2	5	125	7°	1.68	40	Rectangle	0.25
			10°	1.74			0.19
			14°	1.77			0.14

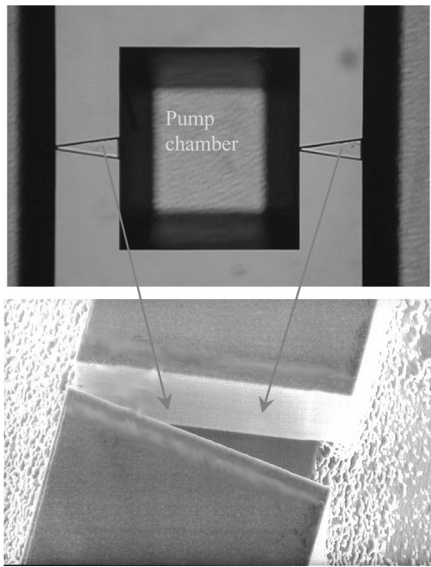


Fig. 3. An optical image of a finished micro diffuser/nozzle pump and an SEM photo of the diffuser/nozzle.

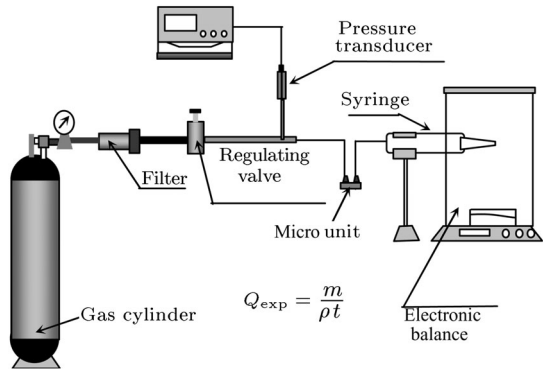


Fig. 4. Schematic diagram of the steady-flow measurement setup.

Stationary flow measurements were performed on both the single diffuser/nozzles and the diffuser/nozzle pump using gas as the working fluid. Our experiment was carried out with low-pressure micro-flow setup at constant temperature, and the simplified diagram of the measurement apparatus was built up as shown in Fig. 4. The experimental setup includes the pressure source, the testing section and the flow rate measuring section. The pressure source consists of a gas cylinder, a filter, and a precise pressure reg-

ulating valve. The testing section consists of a pressure transducer, which is connected to the inlet of the micro-unit used to measure the inlet pressure. The other port of the micro-unit is linked to a horizontal setting syringe, the working gas passed through the micro-unit is gathered in the syringe. Volume flow of the gas is obtained by measuring the volume change of water forced out by the working gas. The investigated pressure range (10, 15, 20, 25, 30 kPa) of the stationary flow measurements approximately matched the diffuser/nozzle flow and pressure drops during one pump cycle.

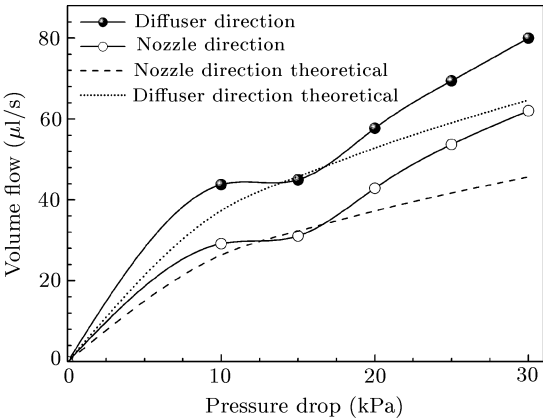


Fig. 5. Gas flow-pressure characteristics for the diffuser/nozzle with length of 125 μm and taper angle of 14° .

The flow rates as a function of gas pressure drop for different diffuser/nozzles were tested firstly. Figure 5 gives the experimental and theoretical curves of the volume flow versus pressure drop for the diffuser/nozzle with the taper angle of 14° and the diffuser/nozzle length of 125 μm . Figure 6 shows the volume flow as a function of pressure drop for a micro diffuser/nozzle pump. Under each pressure drop, the flow rate in diffuser direction is much higher than that in the nozzle direction for both the diffuser/nozzle and the pump, which prove that the diffuser/nozzle and the pump have the ability rectifying the flow direction in the given pressure range of our experiments. For comparison, theoretical calculations of volume flow are also plotted in Fig. 5. It can be seen from Fig. 5 that the errors appear at higher pressure drop, and these uncertainties may be generated by the inaccurate estimation K for regions 1–3, the micro diffuser/nozzle

geometrical characteristics, and the flow measurement conditions (the metrology, the leakage, and the operation conditions).

Figure 7 shows the corresponding calculated relation of diffuser/nozzle flow efficiency ratio η versus pressure drop for the diffuser/nozzles with different taper angles of 7° , 10° and 14° in a fixed length of $125\ \mu\text{m}$, where η is calculated by $\eta = \frac{\xi_{\text{nozz}}}{\xi_{\text{diff}}} = \left(\frac{Q_n}{Q_d}\right)^2$, Q_n and Q_d are measured with the experimental setup shown in Fig. 4. The characteristics of η versus pressure drop for the diffuser/nozzles with different length of $125\ \mu\text{m}$, $90\ \mu\text{m}$ and $70\ \mu\text{m}$ in a fixed taper angle of 14° are depicted in Fig. 8. The flow efficiency ratio η calculated from the experimental results of Fig. 7 are 1.7, 1.5 and 1.7 for the diffuser/nozzles with the taper angle of 14° , 10° , and 7° , respectively. It is demonstrated that the taper angle has no significant effects on the flow efficiency ratio η for rarefied gas

flow in our experimental range and these results are consistent with the theoretical calculations listed in Table 1. For the diffuser/nozzles in Fig. 8, the flow efficiency ratios η are measured to be 1.7, 1.4 and 1.2 with the length of $125\ \mu\text{m}$, $90\ \mu\text{m}$, and $70\ \mu\text{m}$, respectively. The diffuser/nozzle with longer length has a flow efficiency ratio η higher than the diffuser/nozzles with shorter and medium lengths. We think that the differences are due to the entrance and exit effects. A longer diffuser/nozzle can avoid entrance and exit effects more effectively than a shorter one, and therefore make the gas flow fully developed in it. According to the measurement of the diffuser/nozzles the pressure loss coefficients K_{d2} and K_{n2} are calculated to be 1.2 and 0.09, respectively, for the rarefied diffuser/nozzle gas flow. All the experimental data below 15 kPa are abnormal in Figs. 5–8. We think that it is caused by the system error of our measurement setup. Therefore the measured points below 15 kPa should be neglected.

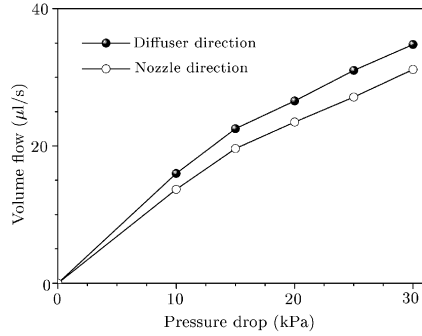


Fig. 6. Gas flow characteristics versus pressure drop for a diffuser/nozzle pump with $L = 125\ \mu\text{m}$, $\theta = 14^\circ$ and $W_1 = 5\ \mu\text{m}$.

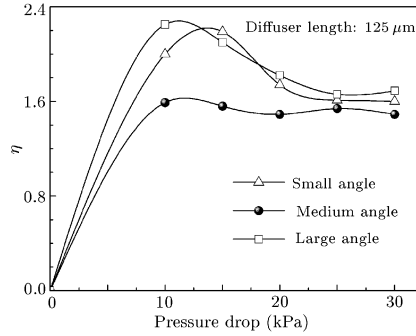


Fig. 7. Measured diffuser/nozzle flow efficiency ratios η as a function of pressure drop for the diffuser/nozzle with three different taper angles 7° , 10° , 14° and in length of $125\ \mu\text{m}$.

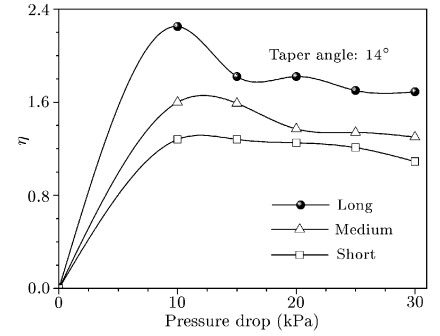


Fig. 8. Measured diffuser/nozzle flow efficiency ratios η as a function of pressure drop for the diffuser/nozzle with three different lengths $125\ \mu\text{m}$, $90\ \mu\text{m}$, $69\ \mu\text{m}$ and in taper angle of 14° .

In summary, we have experimentally investigated the gas flow characteristics in the flat-wall diffuser/nozzles and the pumps with different taper angles and lengths, as a basic research of the diffuser/nozzle micropump. Both the experimental and theoretical results demonstrate that the diffuser/nozzles and the pump could rectify the flow direction under rarefied gas condition. The diffuser/nozzle gains the highest flow efficiency ratio η at the length of $125\ \mu\text{m}$ and the taper angle of 14° . K_{n2} and K_{d2} have been fitted with our experimental results. The excellent flow directing properties of the micro diffuser/nozzle investigated above show that the silicon-based diffuser/nozzle gas micropump is prospective.

References

[1] Mizoguchi H and Ando M et al 1992 *Proceedings of IEEE*

Micro Electro Mechanical Systems Workshop (Travemünde: IEEE) p 31

[2] Zhang C Y et al 2004 *Chin. Phys. Lett.* **21** 1108

[3] Zhang C Y et al 2005 *Chin. Phys. Lett.* **22** 896

[4] Cao B Y et al 2004 *Chin. Phys. Lett.* **21** 1777

[5] Manton M J 1971 *J. Fluid Mech.* **49** 451

[6] Caen R 1979 *Ph.D. Thesis* (Toulouse: INP)

[7] Dorrepaal J M 1993 *J. Fluid Engin.* **118** 464

[8] Aubert C 1999 *Ph.D. Thesis* (Toulouse: INP) p 486

[9] Jin-Ho K et al 2004 *Microelectron. Engin.* **71** 119

[10] Sethu P and Mastrangelo C H 2003 *Sensors and Actuators A* **104** 283

[11] Tsai J H and Lin L W 2002 *J. Microelectromech. Syst.* **11** 665

[12] Studer V, Pepin A, Chen Y and Ajdari A 2002 *Microelectron. Engin.* **61/62** 915

[13] Sun X M et al 2003 *Chin. Phys. Lett.* **20** 2199

[14] Yang K S et al 2004 *J. Micromech. Microengin.* **14** 26

[15] White F M 1986 *Fluid Mechanics* (New York: McGraw-Hill) pp 334 345

[16] Olsson A, Stemme G and Stemme E 1996 *Sensors and Actuators A* **57** 137